ChemComm

Accepted Manuscript

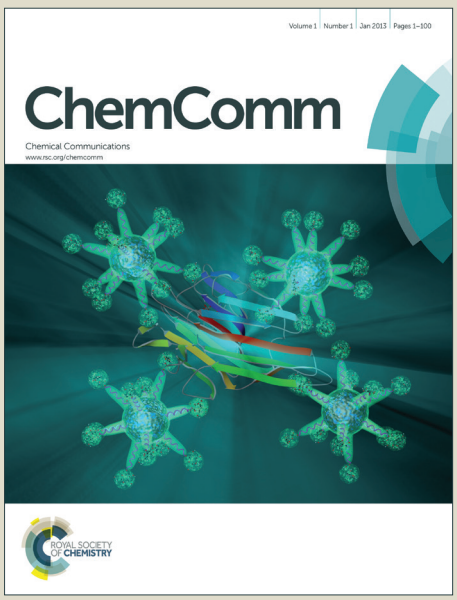

ROYAL SOCIETY OF CHEMISTRY

www.rsc.org/chemcomm

Ultrasensitive Aptamer-based SERS Detection of Cancer Biomarker by Heterogeneous Core-Satellite Nanoassemblies

Wei Ma[#], Honghong Yin[#], Liguang Xu[#], Xiaoling Wu, Hua Kuang[*], Libing Wang, Chuanlai Xu[*]

Received (in XXX, XXX) Xth XXXXXXXXX 201X, Accepted Xth XXXXXXXXX 201X
First published on the web Xth XXXXXXXXX 201X
DOI: 10.1039/b000000x

An ultrasensitive method for surface enhanced Raman scattering (SERS) detection of prostate-specific antigen (PSA) was established based on the aptamer directed core-satellite nanostructures. A limit of detection (LOD) of 4.8 aM for PSA was obtained.

Cancer is a major disease with high mortality, therefore it is very important to achieve an early and sensitive diagnosis to prevent cancer progression. The detection of tumor markers in patient samples is an effective diagnostic method and can lead to treatment of the disease [1-3]. Prostate-specific antigen (PSA), 33-34 KDa glycoprotein, is an organ-specific biomarker, which is found in both normal and diseased prostate cells [4, 5]. The normal cut-off value for PSA level is below 4 ng mL^{-1} in serum, and PSA levels above the cut-off value are generally thought to be associated with prostate cancer [6, 7]. Thus, PSA detection is a critical approach in the diagnosis of prostate cancer.

A large number of methods have been developed for PSA detection, including enzyme-linked immunosorbent assays, electrochemical assays, radioimmunoassay, SERS and etc., are based on the immuno-interaction[8-13]. However, the preparation of antibodies are difficult, expensive and time consuming, and the stability of antibodies is limited for use over a long period. Aptamers are artificial single-strand DNA or RNA screened by systematic evolution of ligands via exponential enrichment [14, 15]. Due to their high affinity to targets, aptamers are regarded as nucleic acid analogues of antibodies[16-19]. Compared with antibodies, chemically synthesized aptamers have numerous advantages, including thermal stability, reusability and easily modificiation, which make them comparable to antibodies [20, 21].

SERS is a promising technique for bio-sensing detection[22-28]. The characteristic spectral signals arise from Raman reporters adsorbed on the surface of SERS substrates, and the enhanced intensity is largely attributed to the high electromagnetic enhancement in narrow gaps between metal nanoparticles (NPs) [29-33]. Importantly, silver NPs showed higher SERS enhancement than gold NPs, which were mostly used as substrates for SERS [34]. Furthermore, strongly plasmonic coupled assemblies are perfect candidates for SERS probes [35, 36].

We designed a novel core-satellite structure comprised of a 17 nm diameter gold core/10 nm thick silver shell NPs (Au@Ag NPs) as core NP and 10 nm diameter Au NPs as satellite NPs. Gandra et al reported core-satellite structures assembled by Au NPs, and demonstrated that these structures had intense electromagnetic hot-spots and are ideal SERS substrates[37]. To further improve the SERS signal, gold nanorods were coated with Ag shell as SERS substrates [38]. In addition, these Ag coated NPs had excellent monodispersity, a consistent shape, and solved the difficult synthesis of larger Ag NPs with homogeneous size.

In this study, the aptamer specific to PSA and its partial complementary DNA were used to assemble core-satellite nanostructures. As shown in Scheme 1, the aptamer modified core NP combined with the complementary DNA coupled to satellite NPs in the absence of PSA. Following the addition of PSA, the aptamer bound the PSA, resulting in the release of satellite NPs from the core NP. The SERS intensity had a direct relationship with the number of satellite NPs around core NP. Therefore, the higher the concentration of PSA, the weaker the Raman intensity. Furthermore, the concentration of PSA could be quantified by the SERS signal.

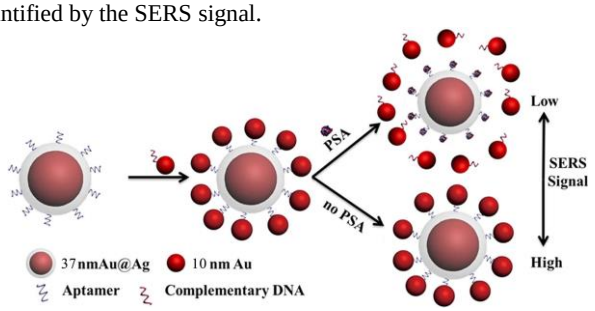

Scheme 1 Scheme of the method for PSA detection based on the aptamer directed core-satellite assemblies.

10 and 17 nm diameter Au NPs were synthesized by the reduction of $HAuCl_4$ using different amounts of trisodium citrate according to a previously published method[39]. 37 nm diameter Au@Ag NPs were synthesized according to the study by Suh[40], which were selected as the SERS substrates and the transmission electron microscopy (TEM) images and ultraviolet-visible (UV-Vis) absorption spectra are shown in Fig. S1 and S2. The modification of DNA onto the NPs was according to the previous method developed by our groups. Core and satellite NPs were functionalized with the apatamers and complementary DNA, respectively. Compared to the bare NPs, the hydrodynamic size of the DNA-modified NPs increased, which demonstrated that DNA was successfully conjugated to the surface of the particles and could be used for the subsequent assembly (Fig. S3). The detailed sequences of the DNA were as follows: Aptamer: 5'-SH-$(T)_{10}$-ATTAAAGCTCGCCATCAAATAGCTGC-3', Complementary DNA: 5'-SH-$(T)_{10}$-GCAGCTATTT-3.

For the assembly of core-satellites nanostructures, 50 μL of core NPs was mixed with 50 μL of satellite NPs in 0.01 M Tris-HCl buffer (50 mM NaCl, 5 mM KCl, 5 mM $MgCl_2$, pH 7.4). After gentle shaking for several minutes, 1 μL of PSA with various concentrations were respectively added to the solutions, resulting in final concentrations of 0, 0.01, 0.05, 0.1, 0.5, 1, 2 and 5 fM. The solutions were then incubated for approximately 8 h at room temperature to form the core-satellite assemblies. Then, 1 μL of Raman reporters (4-nitrothiophenol, 4-NTP) with final concentration of 2 μM was added. Finally, these samples were

analyzed by TEM, DLS, UV-Vis and Raman Spectra.

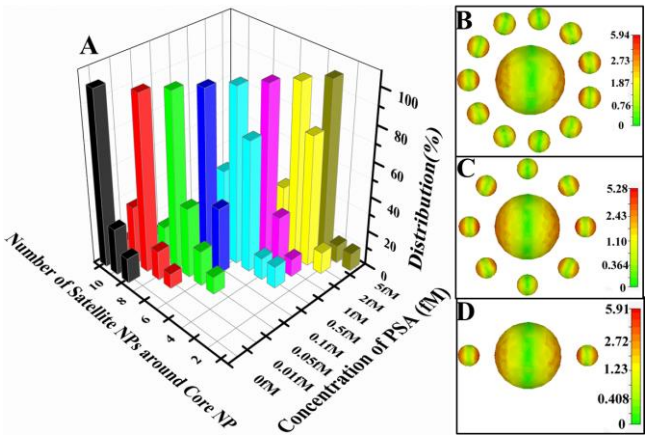

Fig. 1 (A) Statistical analysis of number of satellite NPs around core NP with PSA various concentrations; calculated maps of E-field on the surface of assemblies with eleven (B), eight (C) and two (D) satellite NPs.

At different concentrations of PSA, the representative TEM images are shown in Fig. S4. The sample without PSA had the highest assembly efficiency, and the satellite NPs were completely surrounding core NP. The size of the assembly improved significantly compared with the individual NPs (Fig. S5). With increase the concentration of PSA, the satellite NPs around the core NP decreased gradually. These results were also demonstrated by the statistically average number of Au NPs around the Au@Ag NPs using the TEM images at PSA concentrations of 0, 0.01, 0.05, 0.1, 0.5, 1, 2 and 5 fM (Fig. 1A). The average number of satellite NPs decreased with increased PSA concentration (Fig. 1A and S6).

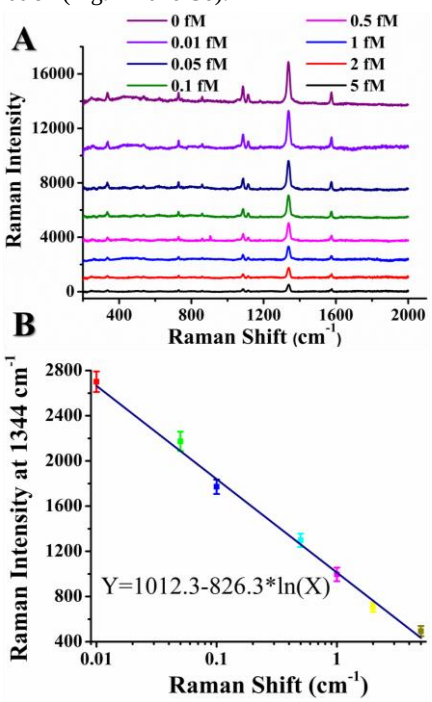

Fig. 2 (A) SERS spectra of 4-NTP in the range of 0-5 fM of PSA. (B) The linear relationship between the concentrations of PSA and the Raman intensity.

To estimate the change in diameter of the core-satellite assemblies, the hydrodynamic sizes of these assemblies at different PSA concentrations were measured using DLS. The typical size distribution of the core-satellite structures is shown in Fig. S7. Following the addition of PSA concentrations ranging from 0 to 5 fM, the size of the assemblies gradually decreased. The change in core-satellite size distribution strongly indicated that the bound of PSA with the aptamer led to the release of satellite NPs from the surface of the core NP. However, the UV-Vis signals at 519 nm and 420 nm showed no obvious change (Fig. S8).

Under optimized conditions, the sensitivity of this sensor was estimated by SERS signals at different PSA concentrations. The SERS intensity of 4-NTP was significantly improved with decreased PSA, which corresponded to the increased assembly of core-satellites. The SERS intensity arose from the total E-field enhancement, which was demonstrated by the surface E-field simulations (Fig.1C-D). When Au NPs numbers increased, the total E-field increased correspondingly. And then, the characteristic SERS peak of 4-NTP at 1334 cm^{-1} was used to quantify the concentration of PSA. As shown in Fig. 2A, the SERS intensity decreased with increased PSA concentrations. The standard curve of PSA detection with an excellent correlation R^2 of 0.9938 was obtained by the SERS signals at 1334 cm^{-1} in the range of 0.01 to 5 fM, and the LOD was calculated to be 4.8 aM (Fig. 2B). Note that the LOD was calculated without PSA giving SERS signal at least three times higher than background.

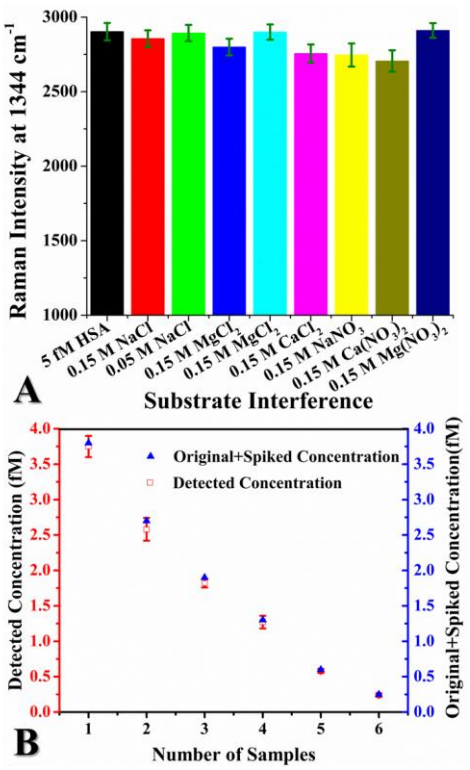

Fig.3 (A) SERS intensity of different substrate interferences based on core-satellite sensors; (B) Correlation ship of original plus spiked PSA concentration (blue symbols) and PSA concentration profiles detected by this developed method (red symbols) the in serum.

To confirm the specificity of this method, the SERS intensity,

in the presence of substrate interference (e.g. human serum albumin (HSA) with different concentrations, ionic strength and electrolyte), was evaluated. As shown in Fig.3A and Fig. S10, the Raman intensity at 1334 cm^{-1} showed no obvious variation with these substrate interference, which confirmed that the PSA specific aptamer did not interact with HSA and plasmonic core-satellite assemblies could not be affected by these substrate interference. Therefore, this method had excellent specificity for the detection of PSA.

The reliability of this sensor was examined by the analysis of PSA in a complex biological matrix, such as serum, which was obtained from the Second Hospital in Wuxi, P.R.C. The samples were diluted to various concentrations including 2.5, 1.8, 1.2, 0.9, 0.5 and 0.2 fM, and were detected by the sensor. As shown in Table S1 and Figure 3B, the recovery was in the range of 95.6%-98.7% to indicate that the sensor was feasible to withstand interferences from multiple substrates present in serum, which is promising for clinical applications

In summary, an ultrasensitive method for PSA detection, utilized the aptamer directed core-satellite assemblies with the strong SERS effect, was developed using SERS signals. As increasing the concentration of PSA, the number of satellite NPs around core NP showed a corresponding decrease, which reduced the SERS signal. This developed method for PSA detection can achieve the LOD of 4.8 aM. This method has significant specificity and practicability, and could be used as a promising technology for the analysis of real samples.

Acknowledgements

This work is financially supported by the National Natural Science Foundation of China (21371081, 21301073).

Notes and references

State Key Lab of Food Science and Technology, School of Food Science and Technology, Jiangnan University, Wuxi, JiangSu, 214122, P. R. China. E-mail: khecho@163.com

#These authors contributed equally to this paper.

† Electronic Supplementary Information (ESI) available: [Nanoparticle Synthesis, Instrumental Characterization, Computer simulation, LOD Cacluation and Corresponding Figures and Tables]. See DOI: 10.1039/b000000x/

1. X. Chen, Y. Ba, L. Ma, X. Cai, Y. Yin, K. Wang, J. Guo, Y. Zhang, J. Chen and X. Guo, *Cell Res.*, 2008, **18**, 997-1006.
2. J. D. Wulfkuhle, L. A. Liotta and E. F. Petricoin, *Nat. Rev. Cancer*, 2003, **3**, 267-275.
3. A. Jemal, T. Murray, E. Ward, A. Samuels, R. C. Tiwari, A. Ghafoor, E. J. Feuer and M. J. Thun, *CA-Cancer J. Clin.*, 2005, **55**, 10-30.
4. H. Lilja, D. Ulmert and A. J. Vickers, *Nat. Rev. Cancer*, 2008, **8**, 268-278.
5. G. Wu, R. H. Datar, K. M. Hansen, T. Thundat, R. J. Cote and A. Majumdar, *Nat. Biotechnol.*, 2001, **19**, 856-860.
6. R. R. Drake, K. Y. White, T. W. Fuller, E. Igwe, M. A. Clements, J. O. Nyalwidhe, R. W. Given, R. S. Lance and O. J. Semmes, *J. Proteomics*, 2009, **72**, 907-917.
7. D. A. Healy, C. J. Hayes, P. Leonard, L. McKenna and R. O'Kennedy, *Ttends Biotechnol.*, 2007, **25**, 125-131.
8. R. de La Rica and M. M. Stevens, *Nat. Nanotechnol.*, 2012, **7**, 821-824.
9. D. S. Grubisha, R. J. Lipert, H.-Y. Park, J. Driskell and M. D. Porter, *Anal. Chem.*, 2003, **75**, 5936-5943.
10. J. Okuno, K. Maehashi, K. Kerman, Y. Takamura, K. Matsumoto and E. Tamiya, *Biosens. Bioelectron.*, 2007, **22**, 2377-2381.
11. H. Graves, N. Wehner and T. A. Stamey, *Clin. Chem.*, 1992, **38**, 735-742.
12. A. Fenner, *Nat. Rev. Urol.*, 2012, **9**, 354-354.
13. R. J. Laffin, D. W. Chan, M. J. Tanasijevic, G. A. Fischer, W. Markus, J. Miller, P. Matarrese, L. J. Sokoll, D. J. Bruzek and J. Eneman, *Clin. Chem.*, 2001, **47**, 129-132.
14. M. Famulok, G. Mayer and M. Blind, *Acc. Chem. Res.*, 2000, **33**, 591-599.
15. S. Jhaveri, M. Rajendran and A. D. Ellington, *Nat. Biotechnol.*, 2000, **18**, 1293-1297.
16. S. Song, L. Wang, J. Li, C. Fan and J. Zhao, *TrAC-Trend. Anal. Chem.*, 2008, **27**, 108-117.
17. H. Xing, N. Y. Wong, Y. Xiang and Y. Lu, *Curr. Opin. Chem. Biol.*, 2012, **16**, 429-435.
18. M. Famulok, J. S. Hartig and G. Mayer, *Chem. Rev.*, 2007, **107**, 3715-3743.
19. W. Ma, H. Yin, L. Xu, Z. Xu, H. Kuang, L. Wang and C. Xu, *Biosen. Bioelectron.*, 2013, **42**, 545-549.
20. C. H. Lu, J. Li, M. H. Lin, Y. W. Wang, H. H. Yang, X. Chen and G. N. Chen, *Angew. Chem. Int. Ed.*, 2010, **49**, 8454-8457.
21. V. Pavlov, Y. Xiao, B. Shlyahovsky and I. Willner, *J. Am. Chem. Soc.*, 2004, **126**, 11768-11769.
22. B. Sharma, R. R. Frontiera, A.-I. Henry, E. Ringe and R. P. Van Duyne, *Mater. Today*, 2012, **15**, 16-25.
23. T.-Y. Liu, K.-T. Tsai, H.-H. Wang, Y. Chen, Y.-H. Chen, Y.-C. Chao, H.-H. Chang, C.-H. Lin, J.-K. Wang and Y.-L. Wang, *Nat. Commun.*, 2011, **2**, doi:10.1038/ncomms1546.
24. M. D. Porter, R. J. Lipert, L. M. Siperko, G. Wang and R. Narayanan, *Chem. Soc. Rev.*, 2008, **37**, 1001-1011.
25. L. Rodríguez-Lorenzo, R. A. Alvarez-Puebla, I. Pastoriza-Santos, S. Mazzucco, O. Stéphan, M. Kociak, L. M. Liz-Marzán and F. J. García de Abajo, *J. Am. Chem. Soc.*, 2009, **131**, 4616-4618.
26. T. Kang, S. M. Yoo, I. Yoon, S. Y. Lee and B. Kim, *Nano Lett.*, 2010, **10**, 1189-1193.
27. K. Kumar âMaiti, *Chem. Commun.*, 2011, **47**, 3514-3516.
28. J.-M. Li, C. Wei, W.-F. Ma, Q. An, J. Guo, J. Hu and C.-C. Wang, *J. Mater. Chem.*, 2012, **22**, 12100-12106.
29. Y. Zhu, H. Kuang, L. Xu, W. Ma, C. Peng, Y. Hua, L. Wang and C. Xu, *J. Mater. Chem.*, 2012, **22**, 2387-2391.
30. L. Rodríguez-Lorenzo, R. A. Alvarez-Puebla, F. J. G. de Abajo and L. M. Liz-Marz án, *J. Phys. Chem. C*, 2009, **114**, 7336-7340.
31. D.-K. Lim, K.-S. Jeon, H. M. Kim, J.-M. Nam and Y. D. Suh, *Nat. Mater.*, 2010, **9**, 60-67.
32. N. Pazos-P érez, S. Barbosa, L. Rodr íguez-Lorenzo, P. Aldeanueva-Potel, J. P érez-Juste, I. Pastoriza-Santos, R. A. Alvarez-Puebla and L. M. Liz-Marz án, *J. Phys. Chem. Lett.*, 2009, **1**, 24-27.
33. W. Ma, M. Sun, L. Xu, L. Wang, H. Kuang and C. Xu, *Chem. Commun.*, 2013, **49**, 4989-4991.
34. J. Zhao, A. O. Pinchuk, J. M. McMahon, S. Li, L. K. Ausman, A. L. Atkinson and G. C. Schatz, *Acc. Chem. Res.*, 2008, **41**, 1710-1720.
35. W. Ma, H. Kuang, L. Xu, L. Ding, C. Xu, L. Wang and N. A. Kotov, *Nat. Commun.*, 2013, **4**, doi:10.1038/ncomms3689.
36. Y. Zhao, L. Xu, L. M. Liz-Marzán, H. Kuang, W. Ma, A. Asenjo-García, F. J. García de Abajo, N. A. Kotov, L. Wang and C. Xu, *J. Phys. Chem. Lett.*, 2013, **4**, 641-647.
37. N. Gandra, A. Abbas, L. Tian and S. Singamaneni, *Nano Lett.*, 2012, **12**, 2645-2651.
38. M. F. Cardinal, B. Rodríguez-González, R. A. Alvarez-Puebla, J. Pérez-Juste and L. M. Liz-Marzán, *J. Phys. Chem. C*, 2010, **114**, 10417-10423.
39. C. J. Loweth, W. B. Caldwell, X. Peng, A. P. Alivisatos and P. G. Schultz, *Angew. Chem. Int. Ed.*, 1999, **38**, 1808-1812.
40. J.-H. Lee, J.-M. Nam, K.-S. Jeon, D.-K. Lim, H. Kim, S. Kwon, H. Lee and Y. D. Suh, *ACS Nano*, 2012, **6**, 9574-9584.